Mitochondrial dysfunction is an early consequence of partial or complete dystrophin loss in *mdx* mice.

Timothy M Moore
University of California Los Angeles
Amanda Lin
University of California Los Angeles
Alexander R Strumwasser
University of California Los Angeles
Kevin Cory
University of California Los Angeles
Kate Whitney
University of California Los Angeles
Theodore Ho
University of California Los Angeles
Timothy Ho
University of California Los Angeles
Joseph L Lee
University of California Los Angeles
Daniel H Rucker
University of California Los Angeles
Christina Q Nguyen
University of California Los Angeles
Aidan Yackly
University of California Los Angeles
Sushil K Mahata
VA San Diego Healthcare System
Jonathan Wanagat
University of California Los Angeles
Linsey Stiles
University of California Los Angeles
Lorraine P Turcotte
University of Southern California Health Sciences Center
Rachelle H Crosbie
University of California Los Angeles
Zhenqi Zhou (zhenqizhou@mednet.ucla.edu)

University of California Los Angeles https://orcid.org/0000-0001-6560-9704

Research

Keywords: Muscular Dystrophy, Mitochondria, Skeletal Muscle, Metabolism, Dystrophin

Posted Date: February 19th, 2020

DOI: https://doi.org/10.21203/rs.2.23961/v1

Abstract

Background:

Muscular dystrophies are a diverse family of genetic and hereditary disorders manifested primarily by the progressive wasting of skeletal muscle. Duchenne muscular dystrophy (DMD), the most common muscular dystrophy, has no cure, with most treatments seeking to mitigate symptoms. Emerging gene or stem cell therapies hold promise, although widespread clinical adoption may not occur for quite some time. There remains a need for alternative strategies, including drug and lifestyle combination-based therapies, and to continue furthering understanding the physiological effects of dystrophin gene mutations. Mitochondrial dysfunction is well known as a pathological feature of DMD. However, whether mitochondrial dysfunction is a cause or the consequence of DMD is not well known. We hypothesized that dystrophin deletion would lead to mitochondrial and metabolic abnormalities prior to the onset of observable muscle damage.

Methods:

Utilizing the commonly employed muscular dystrophy mouse model, C57BL/10ScSn-*Dmd*^{mdx}/*J* (mdx), we sought to determine how the loss of dystrophin effects mitochondria and metabolism in both male and female *mdx* mice. We also treated male *mdx* mice with an autophagy inhibitor, leupeptin, to investigate its potentially impact on *mdx* pathology.

Results:

We detected, via electron microscopy, aberrant mitochondrial morphology, reduced cristae numbers per area of mitochondria, and large mitochondrial vacuoles from both two-week-old male and 24-week-old female *mdx* carrier mice, prior to the onset of visible muscle fiber damage. We systematically characterized mitochondria during disease progression starting before the onset of gross muscle fiber damage noting changes in mitochondrial DNA copy number and regulators of mitochondrial size. We further detected mild metabolic and mitochondrial impairments in female *mdx* carrier mice (heterozygous *mdx*/+) that was exacerbated with high-fat diet feeding. Lastly, we found autophagy inhibition did not improve pathology in *mdx* male mice.

Conclusions:

Our results suggest that prior to the onset of visible muscle damage, mitochondrial and metabolic abnormalities are present within the *mdx* mouse.

Background

Muscular dystrophies are a diverse family of genetic disorders manifesting primarily by the progressive wasting of skeletal muscle. The most severe and frequent muscular dystrophy, Duchenne muscular dystrophy (DMD), is an X-linked disorder caused by mutations in the dystrophin gene and affects

approximately one in every 3,500–5,000 male births (1–3). DMD patients present with clinical manifestations typically before age three with ambulatory loss during teenage years and eventual death before age 30 primarily due to respiratory and cardiac failure (4, 5). Most DMD patients have minimal or no detectable dystrophin at the sarcolemma within muscle (6). The most commonly used mouse model to study DMD is the C57BL/10ScSn-*Dmd*^{mdx}*/J* mouse (*mdx)*„ which possesses a point mutation in exon 23 of the dystrophin coding region leading to a premature stop codon (7). Although the *mdx* mouse manifests the hallmark symptoms of DMD in humans, the phenotype is less severe than in DMD, particularly with respect to the associated cardiomyopathy and respiratory dysfunction that is life-threatening in DMD (8, 9).

Currently, DMD has no cure. Existing clinical care includes corticosteroids that delay disease progression, but frequently produce severe adverse side effects (10–13). Additional developing therapies hold promise, especially those utilizing AAV delivery of microdystrophin, exon skipping via antisense oligonucleotides, or CRISPR-Cas9 gene-editing technology (14, 15). Nevertheless, these therapies have experienced recent setbacks, are often only directed to a specific subset of muscular dystrophy patients, or face several regulatory hurdles (16). While these developments are encouraging, it is likely that such treatments are several years from the accepted standard of care and FDA approval. Therefore, there is a need for alternative strategies, including combination-based therapies, that can be informed from a more complete understanding of the cellular and physiological impact on the myofiber as a consequence of dystrophin loss.

Muscle fibers have a well-ordered intracellular structure that is critical for neural control of force production and load-bearing. Mitochondria within the skeletal muscle are part of this ordered structure, and their specific location within muscle fibers permits the generation of energy in areas of greatest demand (17–19). Recent evidence indicates mitochondria can adapt in size and morphology to changes in the cellular environment in virtually all cell types assessed (20–22). Part of this adaptation includes the formation of new mitochondria (biogenesis), alteration in size and shape (fission and fusion), and removal of damaged or unneeded mitochondria by autophagic turnover (mitophagy) (23, 24). All phases of this adaptation typically occur in unison toward a particular mitochondrial adaptive state. Dysfunction of any adaptive response can lead to dysmorphology, impaired oxidative phosphorylation, metabolic dysfunction, and an inability to adapt to stressors (23, 25–38).

Evidence links muscular dystrophies with mitochondrial and metabolic dysfunction (8, 39–47). However, the timing of these defects with respect to disruption of muscle fiber structure is unknown. We sought to determine the impact of the loss of dystrophin on mitochondrial and metabolic dysfunction in both male and female carrier *mdx* mice. We hypothesized that, due to the highly structured intracellular environment of muscle, lacking a structural protein (dystrophin) would lead to an aberrant mitochondrial and metabolic phenotype. Our results indicate an early mitochondrial and metabolic phenotype in both male and female *mdx* mice prior to the onset of gross muscle fiber abnormalities, potentially suggesting an early mitochondrial role in the etiology of this disease.

Methods

Ethical Approval

The University of California, Los Angeles Institutional Animal Care and Use Committee approved this study. All animal care, maintenance, surgeries, and euthanasia were conducted in accordance with this Institutional Animal Care and Use Committee and the National Institutes of Health.

Muscular Dystrophy Mouse Model

Jackson Laboratories (Bar Harbor, ME, USA) 001801 (genotype: C57BL/10ScSn-*Dmd*^{mdx}*/J)* homozygous female laboratory mice were purchased and crossed with the recommended Jackson 000476 (genotype: C57BL/10ScSnJ) mice (Control) to generate hemizygous male (*mdx)* and female (*mdx* carrier) mice used for all studies. Mice were group-housed two to four per cage, fed chow diet *ad libitum* (8604, Teklad, calories: 25% protein, 14% fat, 54% carbohydrate) or high-fat diet *ad libitum* where indicated (D12451, Research Diets, Inc., calories: 45% fat, 20% protein, 35% carbohydrates), and on a 12-hour light/dark cycle. Mice were fasted for 6 hours prior to euthanasia. LPT (leupeptin) injections were given at 12 mg/kg every other day for five weeks, where indicated in nine-week-old mice.

Glucose and Insulin Tolerance Tests

Glucose and insulin tolerance tests (GTT or ITT) were performed following a 6 hour fast as previously described (48). Briefly, the GTT consisted of an intraperitoneal dextrose (1g/kg) injection and glucose was assessed at 15-minute intervals over the 120-minute testing period. The ITT consisted of an intraperitoneal insulin injection (0.7 U/kg). Blood samples were drawn, and glucose was measured at 0, 15, 30, 45, 60, 90, and 120 minutes post-injection.

Plasma Analysis

Immediately following euthanasia, whole blood was removed via 27-gauge needle from the abdominal aorta and centrifuged at 2,000xG for 2 minutes in EDTA-coated tubes. Plasma was analyzed for insulin and leptin using the Meso Scale Discovery (Rockville, MD, USA) platform following the manufacturer's recommended protocol. Assessment of plasma triglyceride was determined using the L-Type TG M Assay (Wako Diagnostics, Mountain View, CA, USA). Assessment of plasma glucose was determined using HemoCue Glucose 201 Systems glucometer.

Ex vivo Skeletal Muscle Glucose Uptake

Whole-muscle *ex vivo* glucose uptake was assessed using 2-deoxyglucose uptake assay (48). Briefly, soleus muscles were carefully excised from anesthetized animals and immediately incubated for 30 minutes in complete Krebs-Henseleit buffer with or without insulin (60 μU/ml) at 35°C. Muscles were then transferred to the same buffer containing [^{3}H] 2-deoxyglucose (3 μCi/ml) and [^{14}C] mannitol (0.053 μCi/ml), and incubated for 20 minutes before being blotted of excess liquid and frozen in liquid nitrogen.

Muscles were homogenized in lysis buffer and counted for radioactivity. Glucose uptake was standardized to the nonspecific uptake of mannitol and estimated as micromole of glucose uptake per gram of tissue.

Grip strength, Maximal Running Speed, and Dynamic Hanging

The following experiments were performed as previously described without variation (49). Mouse genotypes were blinded to the experimenter for all tests. Grip strength was assessed using the GT3 Grip Strength Meter (BIOSEB, Pinellas Park, FL, USA). Each mouse performed five trials and the highest three trials were averaged. Maximal running speed was assessed as described previously (50). Mice were acclimated to the running treadmill on two separate occasions prior to the maximal running speed test. On testing day, mice performed a 5-minute warm-up at 5–10 m/min. Treadmill speed was increased by 3 m/min until mice were unable to maintain the speed for 10 consecutive seconds with gentle encouragement. Mice were given three attempts at each speed and approximately 60 seconds of rest after each increase in treadmill speed. Dynamic hanging as assessed by latency to fall test, an index of grip strength and muscle endurance, was performed as previously described (51). Mice were acclimated to the wire grid on two separate occasions prior to testing. Mice performed three trials and the data were averaged and reported as a Mean ± SEM. Mice were given five minutes of rest between each trial.

Nucleic Acid Extraction, cDNA Synthesis, and Quantitative RT-PCR

DNA and RNA were extracted from a portion of pulverized frozen muscle using DNeasy/RNeasy Isolation kits (Qiagen, Germantown, MD, USA) as described by the manufacturer. Isolated DNA and RNA were tested for concentration and purity using a NanoDrop Spectrophotometer (Thermo Scientific, Waltham, MA, USA). Isolated RNA was converted into cDNA, assessed for purity, and qPCR of the resulting cDNA levels was performed as previously described (52). All genes were normalized to the housekeeping genes Ppia or 18S. Mitochondrial DNA content was assessed as a ratio of mitochondrial DNA (mtCO2) to nuclear DNA (18S). Primers used for qPCR can be found in Supplemental Table 1.

Immunoblot Analyses

Pulverized frozen muscle was used for immunoblotting. Proteins from each individual whole cell homogenate were normalized (expressed relative to the pixel densitometry) to glyceraldehyde 3-phosphate dehydrogenase (GAPDH, AM4300, Ambion, Foster City, CA, USA). Phosphorylation-specific proteins were normalized (expressed relative to pixel densitometry) to the same unphosphorylated protein (i.e. phosphorylated Drp1 at Ser 616 was expressed relative to the pixel densitometry of Drp1 for each individual sample). See Supplemental Table 2 for a list of the primary antibodies used.

Mitochondrial Isolation

Mitochondria were isolated from muscle via Dounce homogenization and the Mitochondria Isolation Kit for Tissue (Thermo Scientific). Subsequent immunoblotting underwent the same procedure described in the Immunoblot Analyses methods section.

Tissue Histology

Tibialis anterior or gastrocnemius muscles were sectioned and stained for hematoxylin & eosin (H&E), succinate dehydrogenase (SDH), and cytochrome c oxidase (COX) as previously described (53). Semi-quantitative analyses were performed on a blind basis using a scale (high, medium, and low density of staining) for each slide by three individuals.

Transmission Electron Microscopy (TEM)

Soleus muscle was fixed with a freshly prepared fixative containing 2.5% glutaraldehyde and 2% paraformaldehyde in 0.15 M cacodylate buffer. After fixation, muscles were processed for TEM analysis as described previously (54). Ultrathin (~60 nm) sections were viewed using a JEOL 1200EX II (JEOL, Peabody, MA) electron microscope and photographed using a Gatan digital camera (Gatan, Pleasanton, CA) as previously described.

Complex IV Enzyme Activity Assay

Mitochondrial complex IV enzymatic activity was measured using Complex IV Rodent Enzyme Activity Microplate Assay Kit (Abcam, ab109911).

Mitochondrial Respirometry

Frozen skeletal muscle tissues were thawed on ice and homogeneized in MAS (70 mM sucrose, 220 mM mannitol, 5mM KH2PO4, 5 mM MgCl2, 1 mM EGTA, 2 mM HEPES, pH 7.4). The samples were mechanically homogenized with 60 strokes in a teflon-glass dounce homogenizer. All homogenates were centrifuged at 1000×g for 10 min at 4°C then the supernatant was collected. Protein concentration was determined by BCA (Thermo). Homogenates were loaded into Seahorse XF96 microplate in 20 µL of MAS at 6µg/well. The loaded plate was centrifuged at 2,400 x g for 10 min at 4°C (no brake) and an additional 130 µL of MAS supplemented with 100µg/mL cytochrome c was added to each well. Substrate injection were as follows: Port A: NADH (1mM) or succinate + rotenone (5mM + 2 µM); Port B: rotenone + antimycin A (2 µM + 2 µM); Port C: N,N,N',N'-tetramethyl-p-phenylenediamine (TMPD) + ascorbic acid (0.5mM + 1mM); and Port D: azide (50mM). These conditions allow for the determination of the maximal respiratory capacity of mitochondria through Complex I, Complex II, and Complex IV.

Statistical Analysis

Values are presented as mean ± SEM and expressed relative to the average value obtained for each experimental control group unless otherwise stated. Group differences were assessed by Student's t-test with statistical significance established *a priori* at $P < 0.05$ (Graph Pad Prism, San Diego, CA, USA).

Results

Regulators of the mitochondrial life cycle are altered in skeletal muscle from 40-week-old male mdx mice.

DMD was considered to be a disease of metabolic origin with a deficiency of key metabolic systems and regulators, including mitochondria (47). To ascertain the impact of lacking dystrophin upon mitochondria, we first quantified protein and RNA expression for several regulators of the mitochondrial network in gastrocnemius muscles from 40-week-old male mice (*mdx*-40wks), which represents the late, hypertrophic stage of disease. Gene expression for the inflammatory cytokines IFNγ, IL10, IL6, and TNFα were elevated by approximately 4.5 to 7.5 folds in *mdx* males compared with age-matched controls (Figure 1A, $P < 0.05$). We also observed substantial reductions of genes related to mitochondrial fission (*Dnm1l, Mff,* and *Fis1)* and mitophagy (*Maplc3b* and *Pink1)* in *mdx* mice *vs.* age-matched controls (Figure 1A, $P < 0.05$). Reduced phosphorylation of Drp1 at Serine 616, a pro mitochondrial fission signal, and elevated protein levels of mitochondrial fusion regulators (Mfn1 and Mfn2; Figure 1B, Supplemental Figure 1, $P < 0.05$) were evident. Moreover, the protein levels of mitophagy related factors (Parkin and Lc3bI) were also elevated in *mdx* males compared with age-matched controls (Figure 1B, Supplemental Figure 1, $P < 0.05$). In general, we found regulators of mitochondrial life cycle are altered in the skeletal muscle from 40-week-old male *mdx* mice.

Dysfunction of mitochondrial enzymatic activity and morphology are evident at early stages of dystrophin-deficient disease.

Because of the large changes in the expression of regulators of the mitochondrial network observed in late stage of disease (*mdx*-40wks), we hypothesized that these responses resulted from widespread muscle damage and chronic inflammation that eventually causes muscle fiber apoptosis and necrosis. To test this hypothesis, we investigated 11-week-old *mdx* male mice (*mdx*-11wks), which represents the active regeneration phase of the disease (prior to the onset of severe muscle damage, apoptosis, and necrosis) to determine if mitochondrial network alterations occur because of or as a precursor to severe muscle damage as observed previously (55). We found that quadriceps muscle from *mdx*-11wks male mice display reduced mitochondrial DNA copy number as well as reduced mitochondrial DNA derived transcript (mtCO3) relative to age-matched controls (Figure 2A-B, $P < 0.05$). We observed no changes in the gene expression of regulators of mitochondrial DNA replication (*PolGII, Peo1,* and *Mgme1),,* mitochondrial RNA polymerase (*Polrmt),,* and protein translation (*Gfm2;*Figure 2B, $P > 0.05$). At the protein level, several regulators of the mitochondrial network were increased including Lc3bI, Parkin, Pink1, Parl, Mfn2, mature and active Oma1, Fis1, Pgc1α, and Ampkα compared with age-matched controls (Figure 2C, Supplemental Figure 2, $P < 0.05$). Active form of Ampkα (Phosphorylated threonine (Thr) 172) and Drp1 (serine (Ser) 616) were also significantly altered (Figure 2C, Supplemental Figure 2, $P < 0.05$). Since changes in protein levels observed in whole-cell lysates might not reflect proteins present within or on mitochondria, we immunoblotted for a select number of proteins in isolated mitochondria from the quadriceps muscle. Both Parkin and Drp1 were significantly increased, but no change of Mfn2 in the mitochondrial fraction from *mdx*-11wks *vs.* age-matched controls (Figure 2D-F, Supplemental Figure 2, $P < 0.05$) was observed. Electron micrograph images from the soleus muscle depicted a highly altered mitochondria network that included aberrant area, structure, and cristae numbers per area of mitochondria (Figure 2G, $P < 0.05$). Muscle damage was also overtly visible via altered fiber and z-line orientation. As expected, there was extensive myofiber centralized nuclei in mdx samples, which is

consistent with ongoing muscle degeneration and regeneration that is characteristic of DMD (Figure 2H). Such changes occur concomitantly with reduced percentage of muscle fibers with high density of succinate dehydrogenase (SDH) and cytochrome c oxidase (COX) staining indicative of reduced mitochondrial function (Figure 2H).

Mitochondria DNA copy number is reduced at the onset of gross tissue abnormalities in four-week-old mdx male muscles.

Having observed aberrant mitochondria in *mdx* muscle as early as 11 weeks of age, we extended our investigation to four-week-old *mdx* male mice (*mdx*-4wks), which represents the early state of disease just as the first signs of muscle regeneration are evident. Similar to our previous results, we observed a reduction in mitochondrial DNA copy number in quadriceps muscles of *mdx*-4wks vs. age-matched control mice (Figure 3A, $P < 0.05$). Histological staining of gastrocnemius muscle from these same animals revealed muscle fibers with centralized nuclei, localized reductions in fiber cross-sectional area, and regions of nuclei accumulation potentially indicative of inflammatory cell infiltration (Figure 3B). Therefore, even at 4weeks of age, *mdx* muscle exhibits reduced mitochondrial DNA copy number simultaneously with the onset of overt muscle fiber damage.

Mitochondria from prenecrotic two-week-old mdx male muscle displays altered size and cristae structure.

To further test our hypothesis regarding the connection between mitochondria and muscle damage, we generated two-week-old *mdx* male mice (*mdx*-2wks), which represent the prenecrotic stage of disease and is before the onset of overt muscle pathology. We measured mitochondrial DNA copy number in quadriceps muscles and found no difference between *mdx*-2wks and age-matched controls (Figure 4A, $P > 0.05$). Quadriceps muscles were immunoblotted for several proteins related to mitochondria, mitophagy, fission, fusion, and biogenesis which showed no differences in levels of these marker proteins between the two groups (Figure 4B, $P > 0.05$). Gross muscle fiber morphology was examined by histological staining of the gastrocnemius muscle, revealing no signs of muscle damage. In fact, *mdx* and control samples were virtually indistinguishable between *mdx*-2wks and age-matched controls (Figure 4C). Despite observing no differences in mitochondrial DNA copy number, protein levels, and muscle fiber morphology, we found reduced cristae numbers per area of mitochondria and the presence of mitochondrial vacuoles in muscle from two-week-old *mdx* male mice in electron micrographs (Figure 4D). Additionally, although mitochondrial oxygen consumption rate of complex I/II/IV were not altered, mitochondrial complex IV enzymatic activity was significantly decreased (Figure 4E-F). These results suggest the alteration of mitochondrial architecture and enzyme activity before the onset of observable muscle damage.

Autophagy inhibition did not improve muscle or mitochondrial phenotype in mdx male mice.

Our previous results in *mdx* mice at40wks and 11wks of age revealed elevated levels of genes and proteins related to mitophagy and autophagy. Furthermore, electron micrograph images of *mdx*-2wks displayed mitochondrial vacuoles. These observations and other results from the research community

have supported the concept of autophagy inhibition as a potential therapy for muscle wasting conditions (39, 56, 57). Therefore, we treated *mdx* male mice via intraperitoneal injections of saline (*mdx* + saline) or the autophagy inhibitor, leupeptin (*mdx* + LPT) for five weeks, as described previously (58–60), starting at 9 weeks of age in an attempt to preserve mitochondrial degradation. Within quadriceps muscles, mitochondrial DNA copy number was not changed in *mdx* + LPT *vs.* saline-treated *mdx* mice (Figure 5A, $P < 0.05$). Without changing gene expression, LPT treatment elevated the protein level of mitochondrial proteins (Drp1, Vdac1, Opa1, and Complex IV) and mitophagy related factors (Lc3bII/I, p62, and Pink1), validating robust autophagy inhibition by LPT (Figure 5B, Supplemental Figure 3A-B). However, mitochondrial enzymatic histochemical and activity analyses of the tibialis anterior muscle showed no differences in LPT treated animals suggesting LPT treatment did not ameliorate mitochondrial dysfunction in *mdx* mice (Figure 5C-, 5D, $P > 0.05$).

Female asymptomatic mdx carriers present with diet-induced obesity and insulin resistance.

Women who are carriers of the DMD gene are largely asymptomatic with regard to skeletal muscle symptoms, but they are susceptible to cardiomyopathy (61–65). Recent Given that we observed mitochondrial defects in presymptomatic mdx muscle, we sought to query the impact upon mitochondria, muscle, and metabolism in 24-week-old female *mdx* carriers (*mdx* carriers) mice. Female *mdx* carriers were chosen because human female *mdx* carriers typically display symptoms during adult hood and because maximal muscle growth has nearly been achieved according to Jackson laboratory growth curves. We found that female *mdx* carriers displayed similar body weight to age-matched controls (Figure 6A, $P > 0.05$). These mice showed a lower gonadal white adipose tissue mass (gWAT) although no differences in the weights of other metabolic organs (Figure 6B, $P < 0.05$) were observed. Because of the role of muscle in glucose homeostasis, we performed glucose and insulin tolerance tests (GTT and ITT respectively). Female *mdx* carrier mice showed slight impairments in glucose and insulin sensitivity although plasma insulin, leptin, and triglyceride values were not different compared to age-matched controls (Figure 6C-D, Supplemental Figure 4A-C, $P < 0.05$). *Ex vivo* glucose uptake into excised soleus muscles revealed a similar modest reduction in insulin-stimulated glucose uptake in female *mdx* carriers, although this did not reach statistical significance (Figure 6E, $P > 0.05$). We then performed functional muscle strength and endurance testing and found no differences between the two groups in these parameters (Supplemental Figure 4D-F, $P > 0.05$). Our previous results indicated that a loss of dystrophin had an impact upon the expression of regulators of the mitochondria life cycle within skeletal muscle. However, female *mdx* carriers fed with normal chow showed no differences in proteins related to mitophagy, autophagy, mitochondrial biogenesis, fission, or fusion (Figure 6F, $P > 0.05$). Nevertheless, electron micrograph images from female *mdx* carriers consistently displayed mitochondrial vacuoles, similar to what was observed in presymptomatic 2 weeks old *mdx* mice, despite no overt changes to the muscle fiber or z-line orientation (Figure 6G). Moreover, we performed both enzymatic and seahorse assays and observed a significant reduction of mitochondrial complex IV activity in female *mdx* carriers, suggesting a defect in mitochondrial function (Figure 6H-I, $P < 0.05$). Interestingly, we found that high-fat diet (HFD) administration significantly reduced quadriceps and gastrocnemius muscle weights, dramatically elevated body weight, gWAT weight, impaired GTT, and elevated fat mass ratio without

changing plasma triglyceride and lactate levels in female *mdx* carriers (Figure 6 J-L, Supplemental Figure 4G-I, $P < 0.05$). These results suggest female *mdx* carriers present with mild metabolic impairment that is exacerbated with HFD administration.

Discussion

While there are three FDA approved drugs for DMD, there is currently no cure for this disease. It is likely that combinatorial approaches will be needed to address the multi-faceted features of DMD. Thus, a greater understanding of the many consequences of loss of dystrophin are needed in order to inform the rationale design of combinatorial therapies. We sought to understand the biological impact of lacking functional dystrophin protein upon mitochondria and metabolism within male and female mice. We hypothesized that due to the highly structured intracellular environment of muscle, lacking a structural protein (dystrophin) would lead to an aberrant mitochondrial and metabolic phenotype. This, in turn, would exacerbate muscle damage, propagating this vicious cycle.

We utilized the commonly employed *mdx* mouse, where males have little, if any, detectable dystrophin expression and female carriers have a roughly 50% reduction in dystrophin expression due to possessing one mutant copy of the dystrophin gene. We detected, via electron microscopy, aberrant mitochondrial morphology, reduced cristae numbers per area of mitochondria, and large empty spaces within mitochondria in both male and female *mdx* mice prior to the onset of observable muscle fiber damage. To our knowledge, this work represents the first to suggest that mitochondrial ultrastructure is impacted prior to gross muscle fiber damage. We further observed impaired complex IV enzymatic activity. Nevertheless, published research does suggest a mitochondrial phenotype occurring early in muscular dystrophy disease progression (66, 67). These data suggest that a connection may exist between mitochondria, dystrophin, and muscle fiber damage at least in a mouse model of muscular dystrophy. Our results are also in agreement with data showing genetic or pharmacological increases in PGC1α, a known master regulator of mitochondria, improving recovery from injury in *mdx* mice (68–70).

Male *mdx* mice have already been shown to possess metabolic abnormalities after disease onset and during progression (71, 72). We additionally observed mitochondrial dysfunction and metabolic disorder in female *mdx* carrier mice that was exacerbated with high-fat diet feeding. These findings indicate mitochondrial and metabolic dysfunction in female *mdx* carriers with increased susceptibility to diet-induced obesity and insulin resistance despite possessing one functional copy of the dystrophin allele. To our knowledge, this is the first characterization of metabolism and mitochondria within female *mdx* carrier mice. Phenotypic abnormalities, particularly related to mild muscle weakness and cramping, have been noted in a small subset of human female dystrophin mutation carriers (73–79). Nevertheless, epidemiological evidence linking female dystrophin mutation carriers with increased prevalence of obesity, type 2 diabetes, or metabolic dysfunction is lacking. Furthermore, while such metabolic changes are slight in female *mdx* carrier mice, they do suggest that females harboring dystrophin mutations could be susceptible to metabolic dysfunction particularly in the context of diet-induced obesity or aging, which our findings corroborate. Female carriers of DMD may present with associated cardiomyopathy (80),

which has led to more widespread cardiac monitoring of women with DMD offspring. Interestingly, mitophagy has been implicated in DMD cardiac disease (81, 82), further supporting that mitochondria dysfunction is a common feature of DMD.

Our main finding of mitochondrial vacuoles within and adjacent to mitochondria is inconclusive. These structures could represent swollen mitochondria due to calcium influx, enlarged lipid droplets, or autophagic vesicles. Further work is needed to verify the identity of these structures. We found reduced mitochondrial DNA copy number and elevated levels of genes and proteins related to mitophagy and autophagy only in adult *mdx* mice but not in two-week-old *mdx* mice. Lastly, despite the connection between autophagy, mitochondria, and muscular dystrophy (1, 39, 83, 84), autophagy inhibition did not improve disease pathology in adult *mdx* mice, similar to previous results (39, 56, 57, 85). The severity of the disease could preclude the ability of autophagy inhibition to reverse the symptoms. Moreover, the failure of autophagy inhibition to improve the mitochondrial or muscle fiber damage could be related to the relatively low dose administered (12 mg/kg), the method of administration which did not specifically target skeletal muscle (intraperitoneal injection), the infrequent dosing scheme employed (Q. O.D, every other day), or the short duration of administration (five weeks).

Collectively, our results suggest mitochondrial and metabolic abnormalities prior to the onset of observable muscle damage in both male and female *mdx* mice. These results highlight a mitochondrial etiology to the muscular dystrophy family of diseases. Research presented here, as well as from other groups, supports future endeavors to improve mitochondrial function as a component of combination-based therapies to combat muscular dystrophy.

Conclusions

Prior to onset of gross muscle fiber damage, skeletal muscle from male *mdx* and female *mdx* carrier mice presented with aberrant mitochondrial size, shape, reduced cristae numbers per area of mitochondria, and large empty spaces within mitochondria in addition to reduced mitochondrial function. Moreover, female *mdx* carriers present mild metabolic impairments that are exacerbated with high-fat diet feeding. These unexpected phenotypes prior to observable muscle damage suggests a mitochondrial etiology to the muscular dystrophy family of diseases and a connection between mitochondria and the dystrophin protein within muscle. This insight can help shape future therapeutics that might aim to improve mitochondrial function to help mitigate the impact of this devastation group of diseases.

List Of Abbreviations

18S—18S Ribosomal RNA

AMPKa—Protein Kinase AMPK-Activated Catalytic Subunit Alpha 1

AUC—Area under the Curve

CI—Mitochondrial Complex 1 NADH:Ubiquinone Oxidoreductase Subunit B8

CII or II–30—Mitochondrial Complex 2 Succinate Dehydrogenase Complex Iron Sulfur Subunit B

CIII—Mitochondrial Complex 3 Ubiquinol-Cytochrome C Reductase Core Protein II

CIV—Mitochondrial Encoded Cytochrome C Oxidase I

CV or V-a—Mitochondrial Complex 5 ATP Synthase Alpha

COX—Cytochrome C Oxidase

DJ1—Parkinson Disease 7

DNM1L—See Drp1

Drp1—Dynamin Related Protein 1

Esr1—Estrogen Receptor 1

Fis1—Fission, Mitochondrial 1

GAPDH—Glyceraldehyde–3-Phosphate Dehydrogenase

Gastroc - Gastrocnemius

Gfm2—G Elongation Factor Mitochondrial 2

gWAT—Gonadal White Adipose Tissue

H&E—Hematoxylin and Eosin

HSPA1A—Heat Shock Protein Family A Member 1A

HSPA1B—Heat Shock Protein Family A Member 1B

IFNy—Interferon Gamma

IL10—Interleukin 10

IL6—Interleukin 6

JNK1—Mitogen-Activated Protein Kinase 8

LC3B—See MAPLC3B

LPT - Leupeptin

MAPK1—Mitogen-Activated Protein Kinase 1

MAPLC3B—Microtubule Associated Protein 1 Light Chain 3 Beta

*mdx*Duchenne Muscular Dystrophy Mouse Model

MFF—Mitochondrial Fission Factor

MFN1—Mitofusin 1

MFN2—Mitofusin 2

Mgme1—Mitochondrial Genome Maintenance Exonuclease 1

mtCO3—Cytochrome C Oxidase Subunit III

mtDNA—Mitochondrial DNA

Oma1—Overlapping With the M-AAA Protease 1

Opa1—Optic Atrophy Protein 1

Parl—Presenilin Associated Rhomboid Like

Park2—Parkin RBR E3 Ubiquitin Protein Ligase

Peo1—Twinkle mtDNA Helicase

PGC1a—PPARG Coactivator 1 Alpha

Pink1—PTEN Induced Putative Kinase 1

PolGII—DNA Polymerase Gamma 2, Accessory Subunit

Polrmt—RNA Polymerase Mitochondrial

Quad—Quadriceps

Ser - Serine

SDH—Succinate Dehydrogenase

SQSTM1—Sequestosome 1

TFAM—Transcription Factor A, Mitochondrial

Thr - Threonine

Tom20—Translocase of Outer Mitochondrial Member

TNFa—Tumor Necrosis Factor Alpha

wks - weeks

Declarations

Acknowledgements

We would like to thank the UCLA Division of Laboratory Animal Medicine and Katie Moore for assisting us in animal welfare and data collection respectively.

Funding

This research was supported in part by the UCLA Claude Pepper Older Americans Independence Center funded by the National Institute of Aging (5P30AG028748), NIH/NCATS UCLA CTSI Grant (UL1TR000124), and Wellstone NIH NIAMS Center of Excellence Grant (U54 AR052646) to ZZ. TMM was supported by a Kirschstein-NRSA predoctoral fellowship (F31DK108657), a Carl V. Gisolfi Memorial Research grant from the American College of Sports Medicine, a predoctoral graduate student award from the Dornsife College at the University of Southern California, and a post-doctoral fellowship from the UCLA Intercampus Medical Genetics Training Program (T32GM008243). JW was supported by the American Federation for Aging Research, the Glenn Foundation for Medical Research, the UCLA Hartford Center of Excellence, National Institute on Aging Grants AG059847 and AG055518, UCLA Older Americans Independence Center P30 AG028748, UCSD/UCLA Diabetes Research Center Pilot and Feasibility Grant DK063491. LPT was supported by a Gabilan Distinguished Fellowship from the Women in Science and Engineering program at USC. SKM was supported by a grant from the Department of Veterans Affairs (I01BX000323). RHC was supported by NIH R01AR048179 and R01HL126204.

Availability of data and materials

All data generated or analyzed during this study are included in this manuscript and are available upon request.

Author's contributions

The conception and design were performed by TMM & ZZ. The animal experiments, sample collection, and subsequent experimental analysis were conducted by TMM, AJL, ARS, KC, KW, TH, TH, JLL, DHR, CQN, AY, JW, SKM, LPT, LS, RHC & ZZ. The manuscript was originally drafted by TMM & ZZ. All authors contributed to the final drafting of the manuscript.

Ethics approval and consent to participate

The University of California, Los Angeles Institutional Animal Care and Use Committee approved this study. All animal care, maintenance, surgeries, and euthanasia were conducted in accordance with this Institutional Animal Care and Use Committee and the National Institutes of Health.

Consent for publication

Not applicable

Competing Interests

The authors declare that they have no competing interests.

Additional Files

Supplemental Figure 1. Immunoblot images from 40-week-old gastrocnemius muscle.

Supplemental Figure 2. Immunoblot images from 11-week-old quadriceps muscle.

Supplemental Figure 3. Immunoblot images and gene expression results from LPT treated quadriceps muscle. (A) Immunoblots of mitochondrial fission, fusion, mitophagy, and autophagy proteins in quadriceps muscle of *mdx* + saline and *mdx* + LPT (N = 5–6). (B) Gene expression of elevated protein targets in quadriceps muscle of *mdx* + saline and *mdx* + LPT (N = 5–6).

Supplemental Figure 4. Plasma metabolites and muscle strength and endurance measurements. Plasma (A) insulin, (B) leptin, (C) triglyceride of Control and *mdx* carrier fed with normal chow (N = 5–10). (D) Maximum running speed, (E) latency to fall, (F) fore + hindlimb grip strength of Control and *mdx* carrier fed with normal chow (N = 8–10). Plasma (G) triglyceride, (H) lactate, and (I) fat mass/body weight ratio of Control and *mdx* carrier fed with HFD (N = 6–7). *** $P < 0.001$.

Supplemental Table 1. Primers used for qPCR.

Supplemental Table 2. Antibodies used for immunoblotting.

References

1.De Palma C, Perrotta C, Pellegrino P, Clementi E, Cervia D. Skeletal muscle homeostasis in duchenne muscular dystrophy: modulating autophagy as a promising therapeutic strategy. Front Aging Neurosci. 2014;6:188.

2.Govoni A, Magri F, Brajkovic S, Zanetta C, Faravelli I, Corti S, et al. Ongoing therapeutic trials and outcome measures for Duchenne muscular dystrophy. Cell Mol Life Sci. 2013;70(23):4585–602.

3.Emery AE. Clinical and molecular studies in Duchenne muscular dystrophy. Prog Clin Biol Res. 1989;306:15–28.

4.Davies KE, Kenwrick SJ, Patterson MN, Smith TJ, Forrest SM, Dorkins HR, et al. Molecular analysis of muscular dystrophy. J Muscle Res Cell Motil. 1988;9(1):1–8.

5.Pichavant C, Aartsma-Rus A, Clemens PR, Davies KE, Dickson G, Takeda S, et al. Current status of pharmaceutical and genetic therapeutic approaches to treat DMD. Mol Ther. 2011;19(5):830–40.

6.Monaco AP, Bertelson CJ, Liechti-Gallati S, Moser H, Kunkel LM. An explanation for the phenotypic differences between patients bearing partial deletions of the DMD locus. Genomics. 1988;2(1):90–5.

7.Bulfield G, Siller WG, Wight PA, Moore KJ. X chromosome-linked muscular dystrophy (mdx) in the mouse. Proc Natl Acad Sci U S A. 1984;81(4):1189–92.

8.McIntosh LM, Baker RE, Anderson JE. Magnetic resonance imaging of regenerating and dystrophic mouse muscle. Biochem Cell Biol. 1998;76(2–3):532–41.

9.McIntosh LM, Garrett KL, Megeney L, Rudnicki MA, Anderson JE. Regeneration and myogenic cell proliferation correlate with taurine levels in dystrophin- and MyoD-deficient muscles. Anat Rec. 1998;252(2):311–24.

10.Dubowitz V. Prednisone for Duchenne muscular dystrophy. Lancet Neurol. 2005;4(5):264.

11.Muntoni F, Fisher I, Morgan JE, Abraham D. Steroids in Duchenne muscular dystrophy: from clinical trials to genomic research. Neuromuscul Disord. 2002;12 Suppl 1:S162–5.

12.Bushby K, Finkel R, Birnkrant DJ, Case LE, Clemens PR, Cripe L, et al. Diagnosis and management of Duchenne muscular dystrophy, part 1: diagnosis, and pharmacological and psychosocial management. Lancet Neurol. 2010;9(1):77–93.

13.Bushby K, Finkel R, Birnkrant DJ, Case LE, Clemens PR, Cripe L, et al. Diagnosis and management of Duchenne muscular dystrophy, part 2: implementation of multidisciplinary care. Lancet Neurol. 2010;9(2):177–89.

14.Young CS, Hicks MR, Ermolova NV, Nakano H, Jan M, Younesi S, et al. A Single CRISPR-Cas9 Deletion Strategy that Targets the Majority of DMD Patients Restores Dystrophin Function in hiPSC-Derived Muscle Cells. Cell Stem Cell. 2016;18(4):533–40.

15.Marshall JL, Crosbie-Watson RH. Sarcospan: a small protein with large potential for Duchenne muscular dystrophy. Skelet Muscle. 2013;3(1):1.

16.Jones D. Duchenne Muscular Dystrophy awaits gene therapy. Nature Biotechnology. 2019;37:335—7.

17.Bo H, Zhang Y, Ji LL. A mitochondrial cytochrome b mutation causing severe respiratory chain enzyme deficiency in humans and yeast.

18.Anderson S, Bankier AT, Barrell BG, de Bruijn MH, Coulson AR, Drouin J, et al. Sequence and organization of the human mitochondrial genome. Nature. 1981;290(5806):457–65.

19.Bibb MJ, Van Etten RA, Wright CT, Walberg MW, Clayton DA. Sequence and gene organization of mouse mitochondrial DNA. Cell. 1981;26(2 Pt 2):167–80.

20.Lackner LL. Shaping the dynamic mitochondrial network. BMC Biol. 2014;12:35.

21.Liesa M, Palacín M, Zorzano A. Mitochondrial dynamics in mammalian health and disease. Physiol Rev. 2009;89(3):799–845.

22.Twig G, Shirihai OS. The interplay between mitochondrial dynamics and mitophagy. Antioxid Redox Signal. 2011;14(10):1939–51.

23.Twig G, Hyde B, Shirihai OS. Mitochondrial fusion, fission and autophagy as a quality control axis: the bioenergetic view. Biochim Biophys Acta. 2008;1777(9):1092–7.

24.Narendra D, Tanaka A, Suen DF, Youle RJ. Parkin is recruited selectively to impaired mitochondria and promotes their autophagy. J Cell Biol. 2008;183(5):795–803.

25.Pejznochova M, Tesarova M, Hansikova H, Magner M, Honzik T, Vinsova K, et al. Mitochondrial DNA content and expression of genes involved in mtDNA transcription, regulation and maintenance during human fetal development. Mitochondrion. 2010;10(4):321–9.

26.Jornayvaz FR, Shulman GI. Regulation of mitochondrial biogenesis. Essays Biochem. 2010;47:69–84.

27.Miller FJ, Rosenfeldt FL, Zhang C, Linnane AW, Nagley P. Precise determination of mitochondrial DNA copy number in human skeletal and cardiac muscle by a PCR-based assay: lack of change of copy number with age. Nucleic Acids Res. 2003;31(11):e61.

28.Dickinson A, Yeung KY, Donoghue J, Baker MJ, Kelly RD, McKenzie M, et al. The regulation of mitochondrial DNA copy number in glioblastoma cells. Cell Death Differ. 2013;20(12):1644–53.

29.Taanman JW. The mitochondrial genome: structure, transcription, translation and replication. Biochim Biophys Acta. 1999;1410(2):103–23.

30.Scarpulla RC. Metabolic control of mitochondrial biogenesis through the PGC–1 family regulatory network. Biochim Biophys Acta. 2011;1813(7):1269–78.

31.Montgomery MK, Turner N. Mitochondrial dysfunction and insulin resistance: an update. Endocr Connect. 2015;4(1):R1-R15.

32.Westermann B. Mitochondrial fusion and fission in cell life and death. Nat Rev Mol Cell Biol. 2010;11(12):872–84.

33.Seo AY, Joseph AM, Dutta D, Hwang JC, Aris JP, Leeuwenburgh C. New insights into the role of mitochondria in aging: mitochondrial dynamics and more. J Cell Sci. 2010;123(Pt 15):2533–42.

34.Chan DC. Fusion and fission: interlinked processes critical for mitochondrial health. Annu Rev Genet. 2012;46:265–87.

35.Chen H, Vermulst M, Wang YE, Chomyn A, Prolla TA, McCaffery JM, et al. Mitochondrial fusion is required for mtDNA stability in skeletal muscle and tolerance of mtDNA mutations. Cell. 2010;141(2):280–9.

36.Nochez Y, Arsene S, Gueguen N, Chevrollier A, Ferré M, Guillet V, et al. Acute and late-onset optic atrophy due to a novel OPA1 mutation leading to a mitochondrial coupling defect. Mol Vis. 2009;15:598–608.

37.Bach D, Pich S, Soriano FX, Vega N, Baumgartner B, Oriola J, et al. Mitofusin–2 determines mitochondrial network architecture and mitochondrial metabolism. A novel regulatory mechanism altered in obesity. J Biol Chem. 2003;278(19):17190–7.

38.Shen Q, Yamano K, Head BP, Kawajiri S, Cheung JT, Wang C, et al. Mutations in Fis1 disrupt orderly disposal of defective mitochondria. Mol Biol Cell. 2014;25(1):145–59.

39.De Palma C, Morisi F, Cheli S, Pambianco S, Cappello V, Vezzoli M, et al. Autophagy as a new therapeutic target in Duchenne muscular dystrophy. Cell Death Dis. 2012;3:e418.

40.Cole MA, Rafael JA, Taylor DJ, Lodi R, Davies KE, Styles P. A quantitative study of bioenergetics in skeletal muscle lacking utrophin and dystrophin. Neuromuscul Disord. 2002;12(3):247–57.

41.Gulston MK, Rubtsov DV, Atherton HJ, Clarke K, Davies KE, Lilley KS, et al. A combined metabolomic and proteomic investigation of the effects of a failure to express dystrophin in the mouse heart. J Proteome Res. 2008;7(5):2069–77.

42.Even PC, Decrouy A, Chinet A. Defective regulation of energy metabolism in mdx-mouse skeletal muscles. Biochem J. 1994;304 (Pt 2):649–54.

43.Mokhtarian A, Decrouy A, Chinet A, Even PC. Components of energy expenditure in the mdx mouse model of Duchenne muscular dystrophy. Pflugers Arch. 1996;431(4):527–32.

44.Kemp GJ, Taylor DJ, Dunn JF, Frostick SP, Radda GK. Cellular energetics of dystrophic muscle. J Neurol Sci. 1993;116(2):201–6.

45.Khairallah M, Khairallah R, Young ME, Dyck JR, Petrof BJ, Des Rosiers C. Metabolic and signaling alterations in dystrophin-deficient hearts precede overt cardiomyopathy. J Mol Cell Cardiol. 2007;43(2):119–29.

46.Kuznetsov AV, Winkler K, Wiedemann FR, von Bossanyi P, Dietzmann K, Kunz WS. Impaired mitochondrial oxidative phosphorylation in skeletal muscle of the dystrophin-deficient mdx mouse. Mol Cell Biochem. 1998;183(1–2):87–96.

47.Angelin A, Tiepolo T, Sabatelli P, Grumati P, Bergamin N, Golfieri C, et al. Mitochondrial dysfunction in the pathogenesis of Ullrich congenital muscular dystrophy and prospective therapy with cyclosporins. Proc Natl Acad Sci U S A. 2007;104(3):991–6.

48.Ribas V, Drew BG, Zhou Z, Phun J, Kalajian NY, Soleymani T, et al. Skeletal muscle action of estrogen receptor alpha is critical for the maintenance of mitochondrial function and metabolic homeostasis in females. Sci Transl Med. 2016;8(334):334ra54.

49.Moore TM, Zhou Z, Cohn W, Norheim F, Lin AJ, Kalajian N, et al. The impact of exercise on mitochondrial dynamics and the role of Drp1 in exercise performance and training adaptations in skeletal muscle. Mol Metab. 2019;21:51–67.

50.Lerman I, Harrison BC, Freeman K, Hewett TE, Allen DL, Robbins J, et al. Genetic variability in forced and voluntary endurance exercise performance in seven inbred mouse strains. J Appl Physiol (1985). 2002;92(6):2245–55.

51.Mandillo S, Heise I, Garbugino L, Tocchini-Valentini GP, Giuliani A, Wells S, et al. Early motor deficits in mouse disease models are reliably uncovered using an automated home-cage wheel-running system: a cross-laboratory validation. Dis Model Mech. 2014;7(3):397–407.

52.Drew BG, Ribas V, Le JA, Henstridge DC, Phun J, Zhou Z, et al. HSP72 is a mitochondrial stress sensor critical for Parkin action, oxidative metabolism, and insulin sensitivity in skeletal muscle. Diabetes. 2014;63(5):1488–505.

53.Wanagat J, Cao Z, Pathare P, Aiken JM. Mitochondrial DNA deletion mutations colocalize with segmental electron transport system abnormalities, muscle fiber atrophy, fiber splitting, and oxidative damage in sarcopenia. FASEB J. 2001;15(2):322–32.

54.Zhou Z, Ribas V, Rajbhandari P, Drew BG, Moore TM, Fluitt AH, et al. Estrogen receptor α protects pancreatic β-cells from apoptosis by preserving mitochondrial function and suppressing endoplasmic reticulum stress. J Biol Chem. 2018;293(13):4735–51.

55.Ieronimakis N, Hays A, Prasad A, Janebodin K, Duffield JS, Reyes M. PDGFRα signalling promotes fibrogenic responses in collagen-producing cells in Duchenne muscular dystrophy. J Pathol. 2016;240(4):410–24.

56.Childers MK, Bogan JR, Bogan DJ, Greiner H, Holder M, Grange RW, et al. Chronic administration of a leupeptin-derived calpain inhibitor fails to ameliorate severe muscle pathology in a canine model of duchenne muscular dystrophy. Front Pharmacol. 2011;2:89.

57.Selsby J, Pendrak K, Zadel M, Tian Z, Pham J, Carver T, et al. Leupeptin-based inhibitors do not improve the mdx phenotype. Am J Physiol Regul Integr Comp Physiol. 2010;299(5):R1192–201.

58.Haspel J, Shaik RS, Ifedigbo E, Nakahira K, Dolinay T, Englert JA, et al. Characterization of macroautophagic flux in vivo using a leupeptin-based assay. Autophagy. 2011;7(6):629–42.

59.Salminen A. Effects of the protease inhibitor leupeptin on proteolytic activities and regeneration of mouse skeletal muscles after exercise injuries. Am J Pathol. 1984;117(1):64–70.

60.Esteban-Martínez L, Boya P. Autophagic flux determination in vivo and ex vivo. Methods. 2015;75:79–86.

61.Zhong J, Xie Y, Bhandari V, Chen G, Dang Y, Liao H, et al. Clinical and genetic characteristics of female dystrophinopathy carriers. Mol Med Rep. 2019.

62.Florian A, Patrascu A, Tremmel R, Rösch S, Sechtem U, Schwab M, et al. Identification of Cardiomyopathy-Associated Circulating miRNA Biomarkers in Muscular Dystrophy Female Carriers Using a Complementary Cardiac Imaging and Plasma Profiling Approach. Frontiers in Physiology. 2018.

63.Childers MK, Klaiman JM. Cardiac involvement in female carriers of Duchenne or Becker muscular dystrophy. Muscle & Nerve. 2017;55(6):777–9.

64.Viggiano E, Picillo E, Ergoli M, Cirillo A, Del Gaudio S, Politano L. Skewed X-chromosome inactivation plays a crucial role in the onset of symptoms in carriers of Becker muscular dystrophy. The Journal of Gene Medicine. 2017;19(4):e2952.

65.Ishizaki M, Kobayashi M, Adachi K, Matsumura T, Kimura E. Female dystrophinopathy: Review of current literature. Neuromuscular Disorders. 2018;28(7):572–81.

66.Barker RG, Wyckelsma VL, Xu H, Murphy RM. Mitochondrial content is preserved throughout disease progression in the mdx mouse model of Duchenne muscular dystrophy, regardless of taurine supplementation. Am J Physiol Cell Physiol. 2018;314(4):C483-C91.

67.Vila MC, Rayavarapu S, Hogarth MW, Van der Meulen JH, Horn A, Defour A, et al. Mitochondria mediate cell membrane repair and contribute to Duchenne muscular dystrophy. Cell Death Differ. 2017;24(2):330–42.

68.Jahnke VE, Van Der Meulen JH, Johnston HK, Ghimbovschi S, Partridge T, Hoffman EP, et al. Metabolic remodeling agents show beneficial effects in the dystrophin-deficient mdx mouse model. Skelet Muscle. 2012;2(1):16.

69.Selsby JT, Morine KJ, Pendrak K, Barton ER, Sweeney HL. Rescue of dystrophic skeletal muscle by PGC–1α involves a fast to slow fiber type shift in the mdx mouse. PLoS One. 2012;7(1):e30063.

70.Chan MC, Rowe GC, Raghuram S, Patten IS, Farrell C, Arany Z. Post-natal induction of PGC–1α protects against severe muscle dystrophy independently of utrophin. Skelet Muscle. 2014;4(1):2.

71.Strakova J, Kamdar F, Kulhanek D, Razzoli M, Garry DJ, Ervasti JM, et al. Integrative effects of dystrophin loss on metabolic function of the mdx mouse. Sci Rep. 2018;8(1):13624.

72.Blanchet E, Annicotte JS, Pradelli LA, Hugon G, Matecki S, Mornet D, et al. E2F transcription factor–1 deficiency reduces pathophysiology in the mouse model of Duchenne muscular dystrophy through increased muscle oxidative metabolism. Hum Mol Genet. 2012;21(17):3910–7.

73.Brioschi S, Gualandi F, Scotton C, Armaroli A, Bovolenta M, Falzarano MS, et al. Genetic characterization in symptomatic female DMD carriers: lack of relationship between X-inactivation, transcriptional DMD allele balancing and phenotype. BMC Med Genet. 2012;13:73.

74.van Putten M, Hulsker M, Nadarajah VD, van Heiningen SH, van Huizen E, van Iterson M, et al. The effects of low levels of dystrophin on mouse muscle function and pathology. PLoS One. 2012;7(2):e31937.

75.Yoon J, Kim SH, Ki CS, Kwon MJ, Lim MJ, Kwon SR, et al. Carrier woman of Duchenne muscular dystrophy mimicking inflammatory myositis. J Korean Med Sci. 2011;26(4):587–91.

76.Ameen V, Robson LG. Experimental models of duchenne muscular dystrophy: relationship with cardiovascular disease. Open Cardiovasc Med J. 2010;4:265–77.

77.Walcher T, Kunze M, Steinbach P, Sperfeld AD, Burgstahler C, Hombach V, et al. Cardiac involvement in a female carrier of Duchenne muscular dystrophy. Int J Cardiol. 2010;138(3):302–5.

78.Ceulemans BP, Storm K, Reyniers E, Callewaert L, Martin JJ. Muscle pain as the only presenting symptom in a girl with dystrophinopathy. Pediatr Neurol. 2008;38(1):64–6.

79.Hoffman EP, Arahata K, Minetti C, Bonilla E, Rowland LP. Dystrophinopathy in isolated cases of myopathy in females. Neurology. 1992;42(5):967–75.

80.Florian A, Rösch S, Bietenbeck M, Engelen M, Stypmann J, Waltenberger J, et al. Cardiac involvement in female Duchenne and Becker muscular dystrophy carriers in comparison to their first-degree male relatives: a comparative cardiovascular magnetic resonance study. Eur Heart J Cardiovasc Imaging. 2016;17(3):326–33.

81.Kang C, Badr MA, Kyrychenko V, Eskelinen EL, Shirokova N. Deficit in PINK1/PARKIN-mediated mitochondrial autophagy at late stages of dystrophic cardiomyopathy. Cardiovasc Res. 2018;114(1):90–102.

82.Kyrychenko V, Poláková E, Janíček R, Shirokova N. Mitochondrial dysfunctions during progression of dystrophic cardiomyopathy. Cell Calcium. 2015;58(2):186–95.

83.Whitehead NP. Enhanced autophagy as a potential mechanism for the improved physiological function by simvastatin in muscular dystrophy. Autophagy. 2016;12(4):705–6.

84.Piras A, Boido M. Autophagy inhibition: a new therapeutic target in spinal muscular atrophy. Neural Regen Res. 2018;13(5):813–4.

85.Sandri M, Coletto L, Grumati P, Bonaldo P. Misregulation of autophagy and protein degradation systems in myopathies and muscular dystrophies. J Cell Sci. 2013;126(Pt 23):5325–33.

Figures

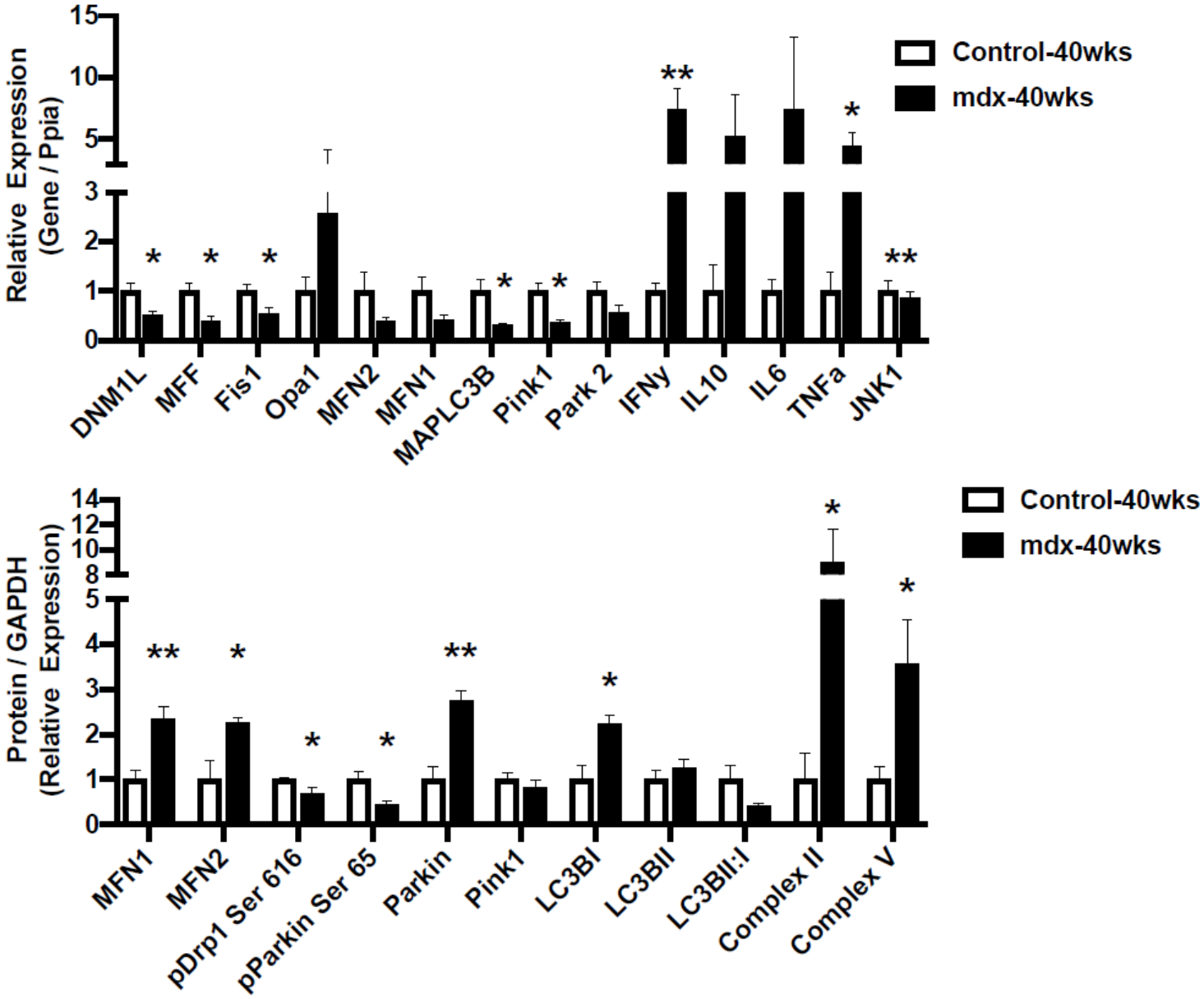

Figure 1

40-week-old mdx male muscles display altered regulators of the mitochondrial life cycle. (A) Gene expression from gastrocnemius muscle (N=4-5). (B) Protein expression from gastrocnemius muscle (N=4-5). Data presented as Mean ± SEM. *, ** P < 0.05, 0.01 respectively.

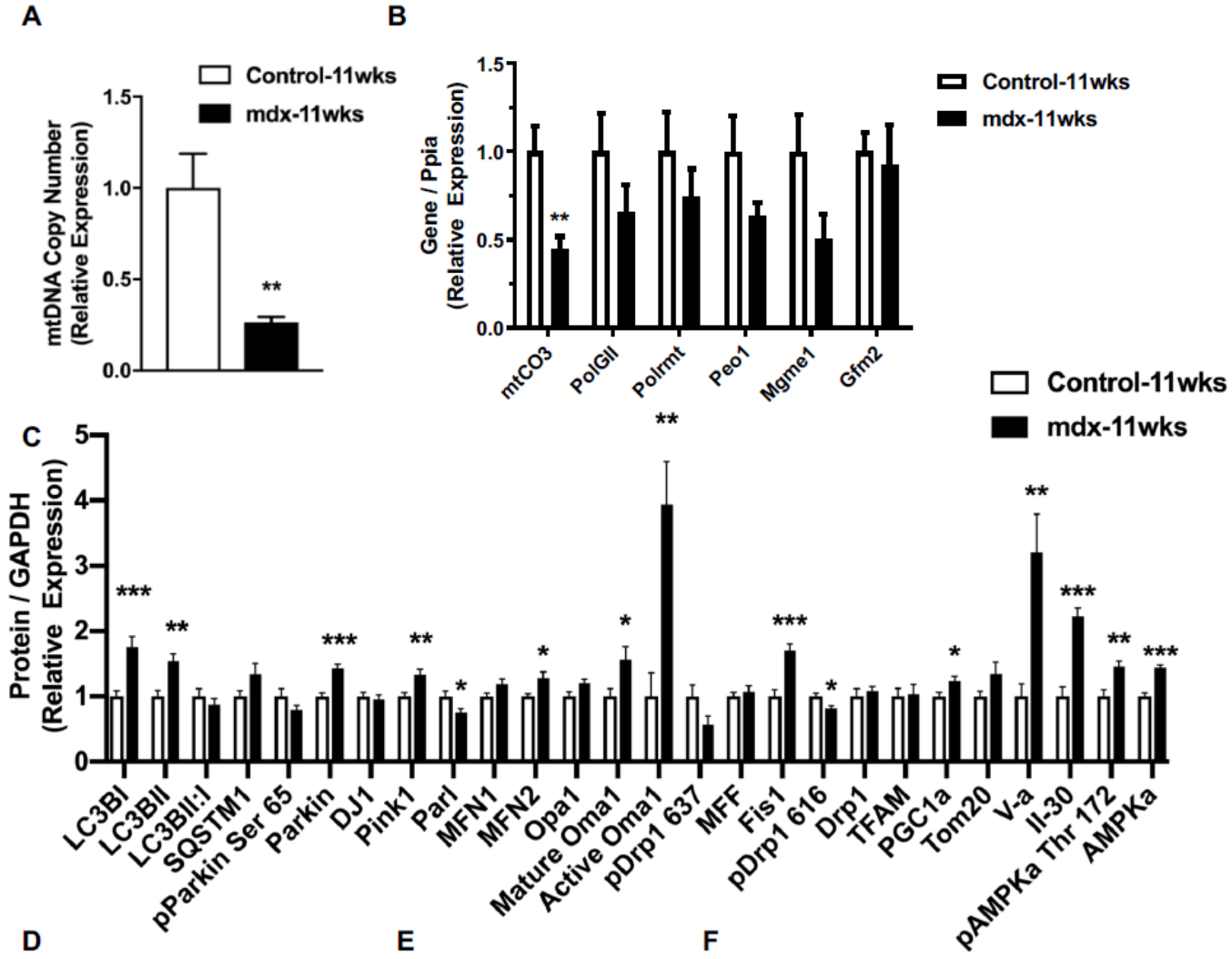

Figure 2

11-week-old mdx male muscles display altered regulators of the mitochondrial life cycle, enzymatic activity, and mitochondrial shape. (A) Mitochondrial DNA copy number in quadriceps muscle (N=6-8). (B) mRNA expression in quadriceps muscle (N=5-8). (C) Protein expression in quadriceps muscle (N=6-8) (D-F) Protein expression in mitochondria isolated from quadriceps muscle (N=6-8). (G) Electron micrograph images of the soleus muscle with quantified mitochondrial area and cristae numbers per area of mitochondria shown right. (H) H&E, SDH, and COX staining in tibialis anterior muscle with the percentage of muscle fiber density shown right (N=13). Black arrow indicates fibers with centralized nuclei. Only some fibers are indicated. Scale bar = 0.1 mm. Data presented as Mean ± SEM. *, **, *** P < 0.05, 0.01, 0.001 respectively.

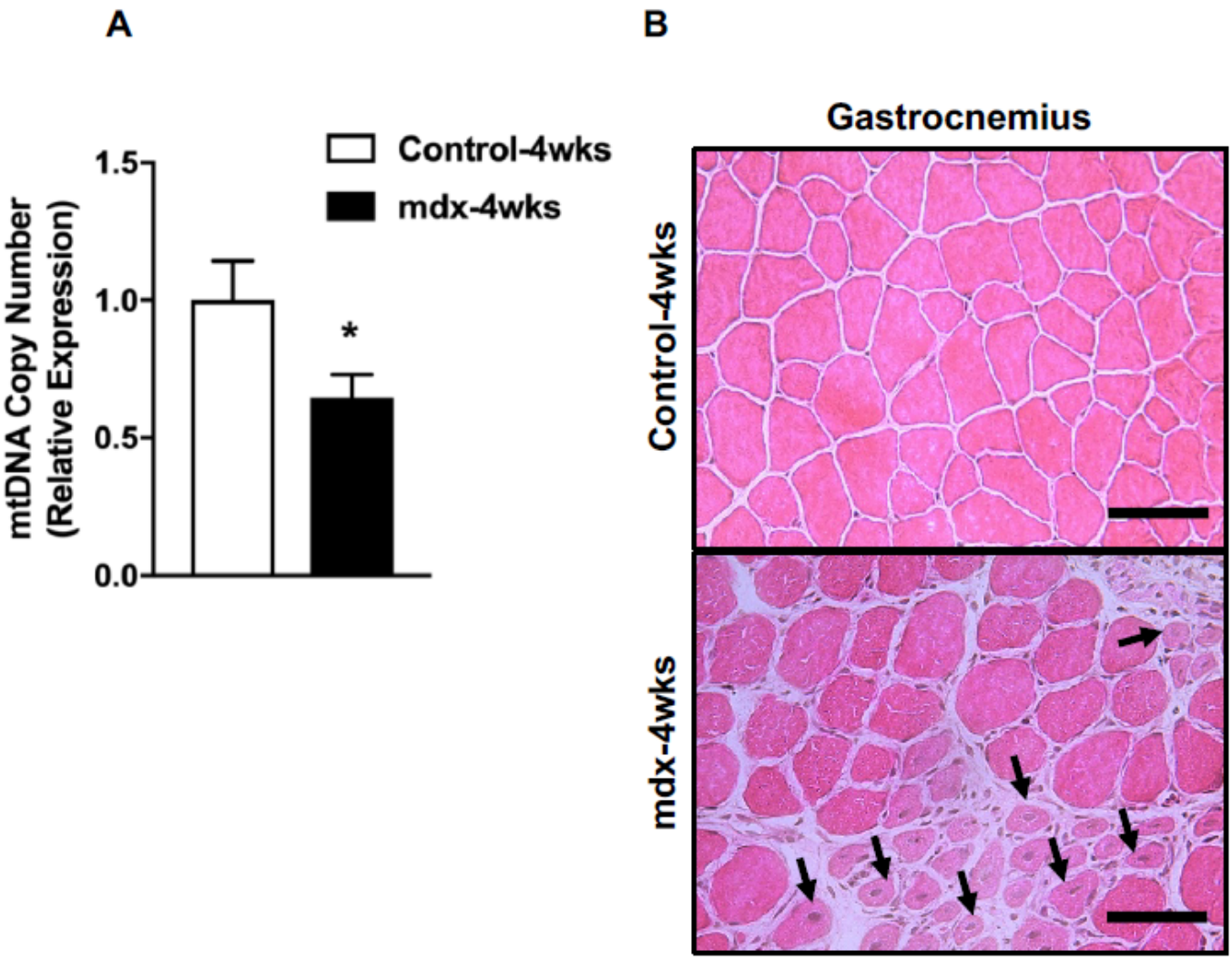

Figure 3

Mitochondria DNA copy number is reduced at the onset of gross tissue abnormalities in four-week-old mdx male muscles. (A) Mitochondrial DNA copy number in quadriceps muscle (N=8-10). (B) H&E stain of gastrocnemius muscle. Black arrows indicate fibers with centralized nuclei. Only some fibers are indicated. Scale bar = 0.1 mm. Data presented as Mean ± SEM. * $P < 0.05$.

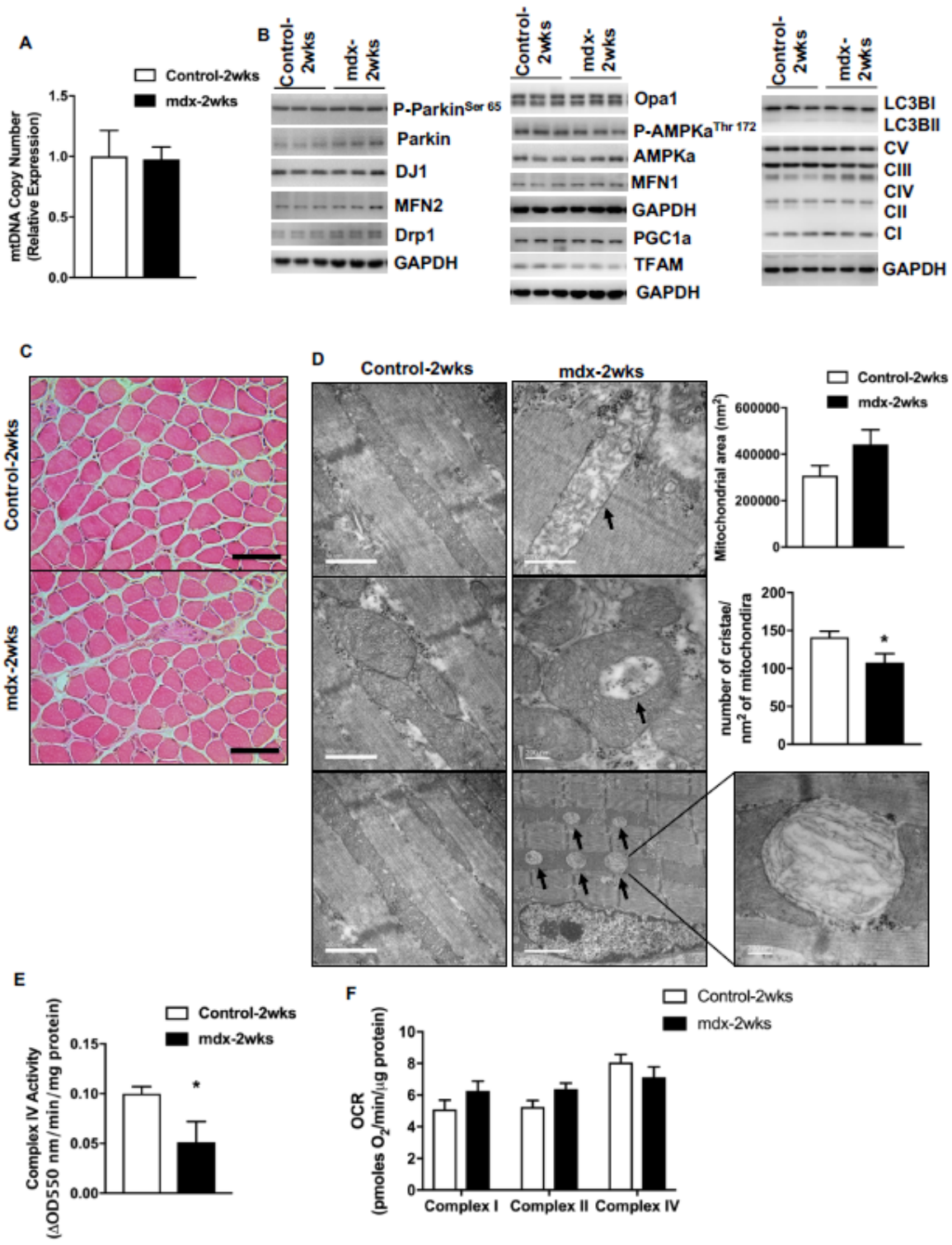

Figure 4

Mitochondria from two-week-old mdx male muscles display altered size, cristae numbers per area of mitochondria, and enzymatic activity. (A) Mitochondrial DNA copy number in quadriceps muscle (N=3-5). (B) Immunoblot images from quadriceps muscle (N=6-8, Showing N=3). (C) H&E stain of gastrocnemius muscle. Scale bar = 0.1 mm. (D) Electron micrograph images of the soleus muscle with quantified mitochondrial area and cristae numbers per area of mitochondria shown right. Black arrows indicate

aberrant mitochondria. (E) Complex IV activity in quadriceps muscle (N=5). Data presented as Mean ± SEM. (F) Mitochondrial respirometry analysis in frozen quadriceps muscle (N=6-8).

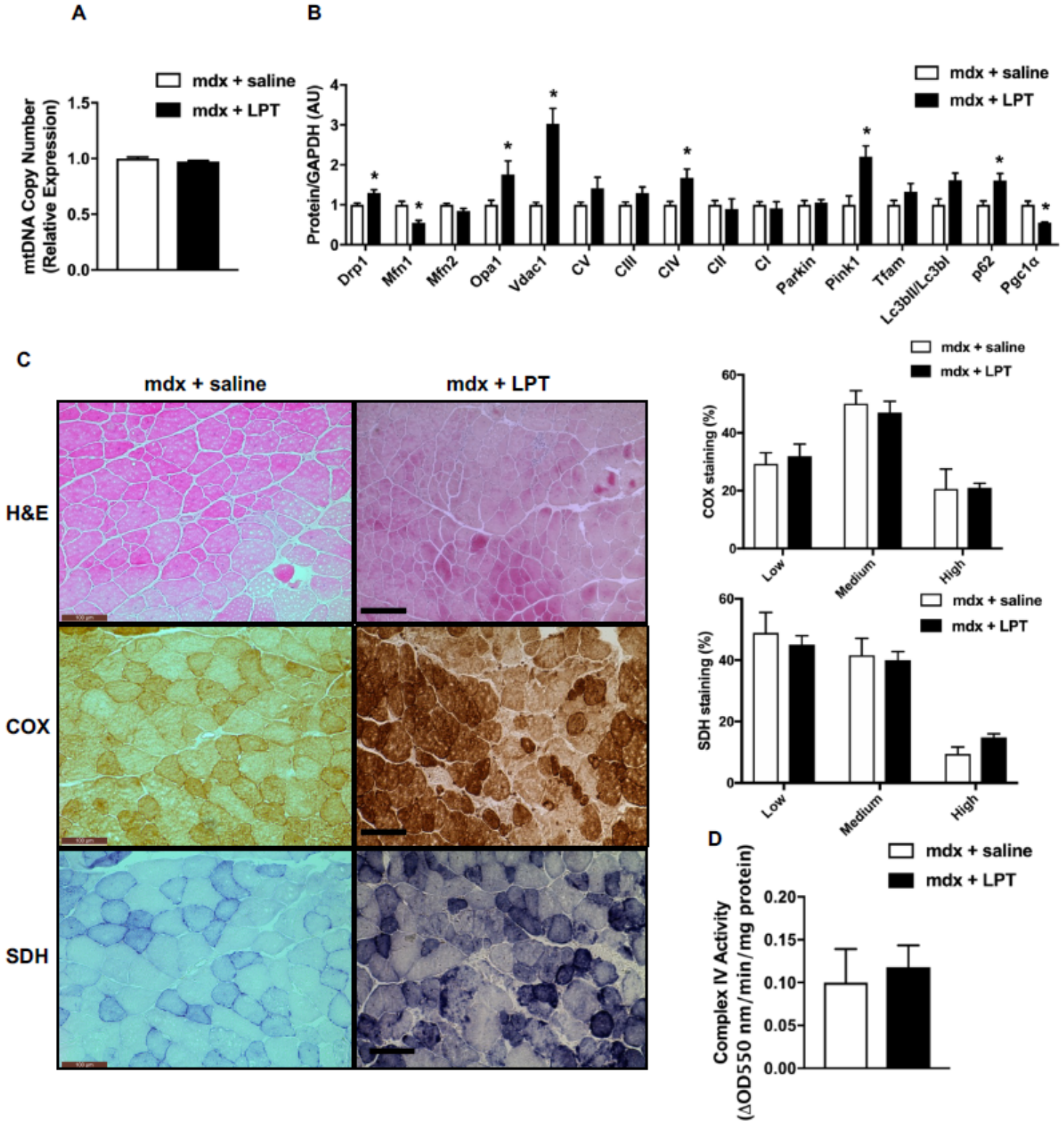

Figure 5

Autophagy inhibition did not improve mitochondrial phenotype in 14-week-old mdx male mice. (A) Mitochondrial DNA copy number in quadriceps muscle (N=5). (B) Protein expression in quadriceps muscle (N=5) (C) H&E, COX, and SDH staining in tibialis anterior muscle with the percentage of muscle

fiber density shown right (N=12). Scale bar = 0.1 mm. (D) Complex IV activity in quadriceps muscle (N=5). Data presented as Mean ± SEM. * P < 0.05.

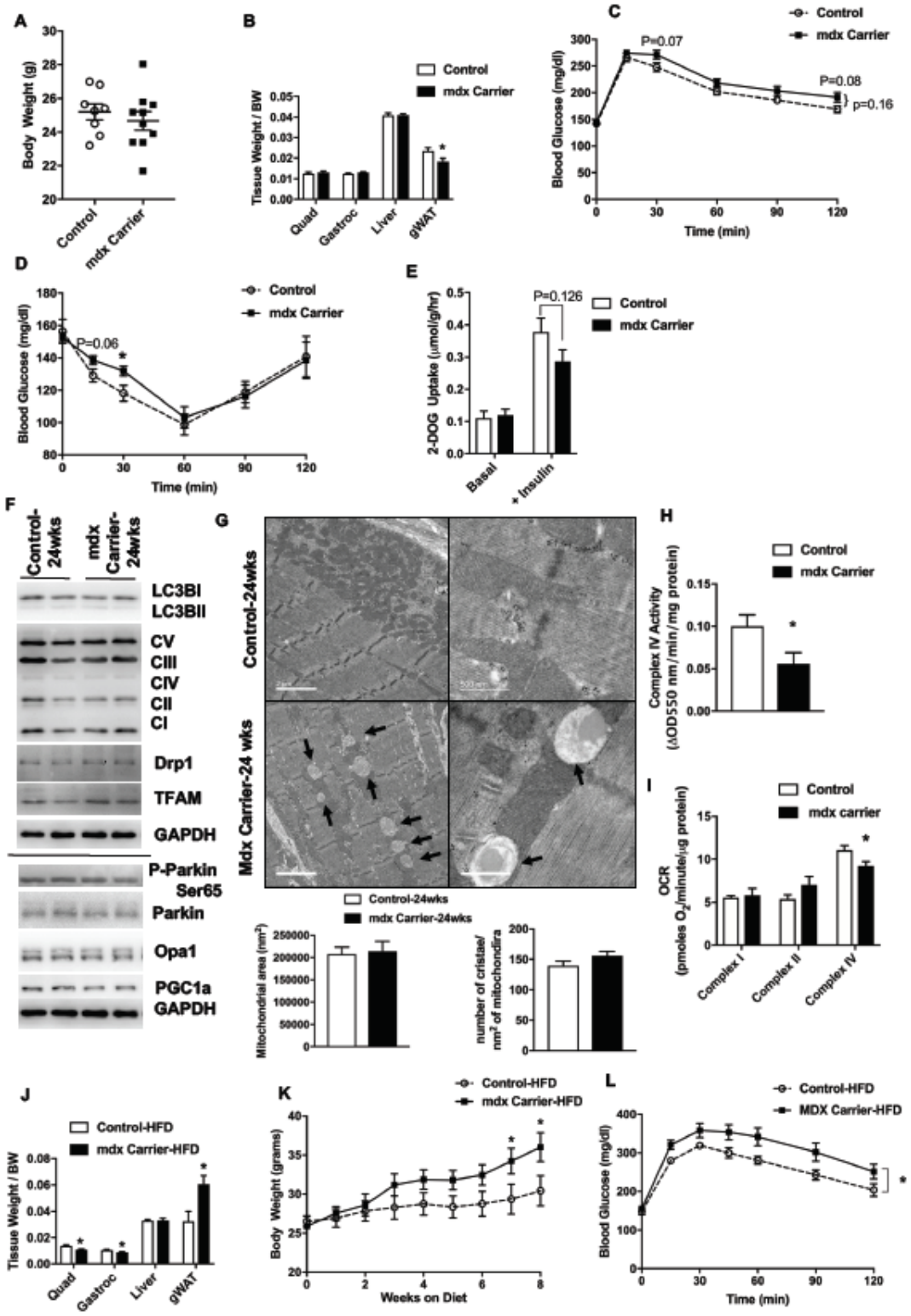

Figure 6

Female mdx carriers present mild metabolic impairments that are exacerbated with high-fat diet feeding. Female mdx carriers fed with normal chow (A-I): (A) Tissue weight relative to body weight. (B) Body weight (grams). (C-D) Glucose and insulin tolerance tests with Area Under the Curve (AUC) insert. (E) 2-

deoxyglucose uptake with or without insulin in excised soleus muscle. (F) Immunoblot images for respective proteins (Showing N=2). (G) Electron micrograph images of the soleus muscle with quantified mitochondrial area and cristae numbers per area of mitochondria shown bottom. Black arrow indicates mitochondrial vacuoles. (H) Complex IV activity in quadriceps muscle (N=5). (I) Mitochondrial respirometry analysis in quadriceps muscle (N=4-6). Female mdx carriers fed with high-fat diet (J-L): (J) Tissue weight relative to body weight. (K) Body weight during high-fat diet feeding. (L) Glucose tolerance tests with Area Under the Curve (AUC) insert. Data presented as Mean ± SEM. * $P < 0.05$.

Supplementary Files

This is a list of supplementary files associated with this preprint. Click to download.

- SupplementalFigure4.pdf
- SupplementalFigure1.pdf
- SupplementalFigure3.pdf
- SupplementalFigure2.pdf
- SupplementalTable1.xlsx
- SupplementalTable2.xlsx